Spurious Symmetry Enhancement in Linear Spin Wave Theory and Interaction-Induced Topology in Magnons

Matthias Gohlke,[1] Alberto Corticelli,[2] Roderich Moessner,[2] Paul A. McClarty,[2] and Alexander Mook[3]
[1]*Theory of Quantum Matter Unit, Okinawa Institute of Science and Technology Graduate University, Onna-son, Okinawa 904-0495, Japan*
[2]*Max Planck Institute for the Physics of Complex Systems, Nöthnitzer Straße 38, 01187 Dresden, Germany*
[3]*Institute of Physics, Johannes Gutenberg University Mainz, 55128 Mainz, Germany*

(Received 15 November 2022; revised 6 September 2023; accepted 3 October 2023; published 31 October 2023)

Linear spin wave theory (LSWT) is the standard technique to compute the spectra of magnetic excitations in quantum materials. In this Letter, we show that LSWT, even under ordinary circumstances, may fail to implement the symmetries of the underlying ordered magnetic Hamiltonian leading to spurious degeneracies. In common with pseudo-Goldstone modes in cases of quantum order by disorder these degeneracies tend to be lifted by magnon-magnon interactions. We show how, instead, the correct symmetries may be restored at the level of LSWT. In the process we give examples, supported by nonperturbative matrix product based time evolution calculations, where symmetry dictates topological features but where LSWT fails to implement them. We also comment on possible spin split magnons in MnF_2 and similar rutiles by analogy to recently proposed altermagnets.

DOI: 10.1103/PhysRevLett.131.186702

From Néel order in the mid 20th century to skyrmion phases in the 21st, magnetically ordered materials have been a constant source of insights into the collective behavior of matter. The coherent spin wave excitations, or magnons, about these magnetic textures provide invaluable information about magnetic structures and couplings. They are also interesting in their own right: as a window into many-body interactions and quasiparticle breakdown [1], as a platform for investigating band topology [2–4], and as an essential ingredient in the functioning of many spintronics devices [5].

One of the most useful theoretical tools at our disposal to understand magnons is an expansion in powers of inverse spin S based on the Holstein-Primakoff bosonization of quantum spins [6]. The single particle spectrum arising from spin wave theory to quadratic order (called linear, or noninteracting, spin wave theory) is often used with great success to constrain magnetic couplings from experimental data. This theory is known to fail qualitatively in cases where coupling between single and multiparticle states becomes important, e.g., in highly frustrated magnets and noncollinear spin textures [1,7,8] and close to quantum phase transitions [9].

Another, more subtle way in which linear spin wave theory (LSWT) can fail qualitatively is called order by disorder [10–13] where spurious ground states and symmetry enhancement exist at the semiclassical level that are lifted by fluctuations. In some instances of quantum order by disorder, a spurious continuous symmetry forces the presence of a pseudo-Goldstone mode in LSWT where none should be present [14]. In this Letter, we focus on a related instance of this physics where, instead of failing to capture degeneracy breaking in the ground state, the LSWT instead does not fully capture symmetries that affect degeneracies higher up in the excitation spectrum [15]. In essence we note that the Landau theory in cases of order by disorder has spurious symmetries and it is the task of this Letter to establish whether finite energy physics can also fail to implement symmetries. With growing interest in magnon band topology [16–36], there is additional impetus to understand how to implement symmetries correctly in LSWT as these provide important constraints on the possible topological band structures that can arise [15,37,38].

Overview.—The cases we consider fall into two classes [see Fig. 1(a)]. The first class is where the lattice symmetries are not manifest for exchange couplings between moments out to nth nearest neighbors but where the symmetries do manifest for longer-range couplings. This, we call the "shell anomaly." Such a situation may be completely physical and, far from being confined to spin wave theory, it may arise in general tight-binding models. The second class is more subtle: where LSWT does not capture certain kinds of exchange anisotropy or "anisotropy blindness." Then, LSWT fails to produce the correct magnon spectrum at a qualitative level and spurious symmetry-protected topological magnon degeneracies occur. We show that degeneracy breaking occurs by carrying out density matrix renormalization group plus matrix product operator time evolution (DMRG + tMPO) [39–41] to resolve band splittings nonperturbatively. While the most straightforward LSWT does not capture the symmetries of the magnetic Hamiltonian, one may show that the symmetry breaking terms, treated

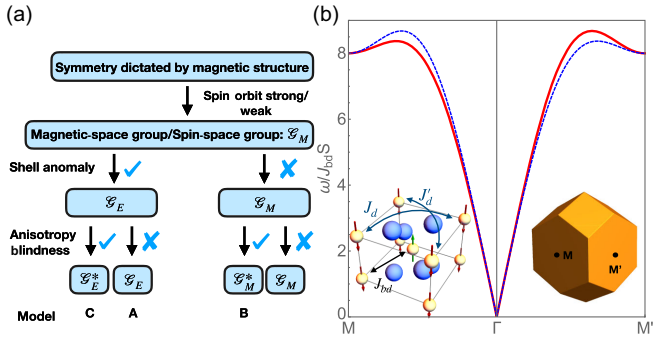

FIG. 1. (a) Flow chart indicating the actual and spurious symmetries that may arise in LSWT. The parent symmetry group $\mathcal{G}_M$ constrained by the lattice symmetries, magnetic structure, and the nature of the exchange may be enhanced via a *shell anomaly* and/or *anisotropy blindness* to new symmetry groups denoted $\mathcal{G}_E^{(*)}$ or $\mathcal{G}_M^*$. (b) Spin wave spectrum for model A exhibiting a shell anomaly in the form of a double degeneracy in the absence of further neighbor terms. The spectrum shown (for the lattice model in the inset) has $J_d \neq J'_d$.

perturbatively, lead to effective magnon hopping terms that do resolve spurious degeneracies. This fact leads us to propose a general solution to the problem by including all symmetry-allowed exchange couplings out to some shell.

Figure 1(a) is a schematic overview of the Letter from a symmetry perspective. If the symmetry group dictated by the lattice, the magnetic ground state, and the presence or absence of exchange anomalies is $\mathcal{G}_M$, the symmetries may be enhanced by the shell anomaly (model A), anisotropy blindness (model B), or both (model C), leading to new symmetry groups. The models A, B, and C are discussed below and serve as worked examples that make contact with material classes such as altermagnets [42,43], chiral magnets [44], and Van der Waals magnets [45].

Shell anomaly and connection to altermagnetism.—We start with an example that illustrates the shell anomaly (model A). Figure 1(b) shows the crystal and magnetic structure of MnF_2. The symmetries ensure that there is a single nearest neighbor coupling $J_{\rm bd}$ on all the bonds joining the two magnetic sublattices in a primitive cell. In MnF_2 this is antiferromagnetic and, for this coupling alone, the model is identical to the simple body-centered tetragonal antiferromagnet with a double (spin) degeneracy in the magnon spectrum. However, further neighbor exchange will, in general, lift the double degeneracy [see Supplemental Material (SM) [46] for details]. Specifically, if the further neighbor couplings J_d and J'_d are unequal, as is allowed by the symmetry of the lattice including the fluoride ion positions, the magnon bands are nondegenerate [cf. Fig. 1(b)]. In this instance, not only the linear theory but in fact the exact spin wave theory has an enhanced symmetry at the nearest neighbor level that is lifted by further neighbor couplings. This splitting—also expected in isostructural materials [60]—is identical to the zero spin-orbit coupled electronic d-wave spin splitting reported in Refs. [42,43,61] that goes under the name "altermagnetism."

In the language of group theory introduced above, the nearest neighbor model has a spurious sublattice symmetry present in $\mathcal{G}_E$ and absent in the full symmetry group $\mathcal{G}_M$. A shell anomaly may occur in materials where the exchange couplings are strictly short range. It is problematic when the exchange couplings in the material break down these symmetries but where this fact is overlooked by the choice of model.

We note that it is possible for further neighbor couplings to be negligible in real materials such that symmetry enhanced degeneracies are present up to instrumental resolution. For example, in the case of MnF_2 inelastic neutron data reveals no degeneracy breaking and, thus, the shell anomaly is active in this material to within instrumental resolution [46,62,63].

Anisotropy blindness.—We now describe the origin of anisotropy blindness. Consider the bilinear magnetic couplings $J_{ij}^{\alpha\beta}$ between moments labeled by i and j with respective components α and β in the quantization frame. Since LSWT is formulated in terms of the transverse spin fluctuations, transverse-longitudinal components $J_{ij}^{z\pm}$ do not enter into the theory. But, for example, the magnetic Hamiltonian with these couplings may have lower symmetry than the Hamiltonian without them. In such a situation, one can generally expect that LSWT will fail to capture certain instances of degeneracy breaking in the magnon spectrum.

This problem may be resolved by computing the dynamical structure factor to higher order in perturbation theory. In particular, the $J_{ij}^{z\pm}$ lead to cubic vertices. Then, bubble diagrams with a pair of such vertices dress the single magnon propagator restoring the correct symmetry of the magnon spectrum. While simple in principle, this is burdensome in practice. Taking model B as an example, we show how the correct symmetries can be implemented instead already on the level of LSWT within a real-space perturbation theory, as verified by the nonperturbative DMRG + tMPO.

Model B: Honeycomb lattice antiferromagnet.—We consider the honeycomb lattice spin-1/2 model with nearest neighbor Heisenberg coupling and interfacial Dzyaloshinskii-Moriya interaction (DMI); see inset in Fig. 2(a). The Hamiltonian is

$$H = \frac{1}{2}\sum_{\langle ij\rangle}[J_z S_i^z S_j^z + J(S_i^x S_j^x + S_i^y S_j^y) + \boldsymbol{D}_{ij}\cdot \boldsymbol{S}_i \times \boldsymbol{S}_j], \qquad (1)$$

with $J_z > J > 0$ being antiferromagnetic and $\boldsymbol{D}_{ij} = D\hat{\boldsymbol{z}} \times \hat{\boldsymbol{e}}_{ij}$; $\hat{\boldsymbol{e}}_{ij}$ is a unit vector along bond direction and $\hat{\boldsymbol{z}}$ along the lattice normal. For $J_z \gg J$ the strong easy-axis Ising anisotropy stabilizes the Néel ground state. The full model with group $\mathcal{G}_M$ has only discrete symmetries whereas the

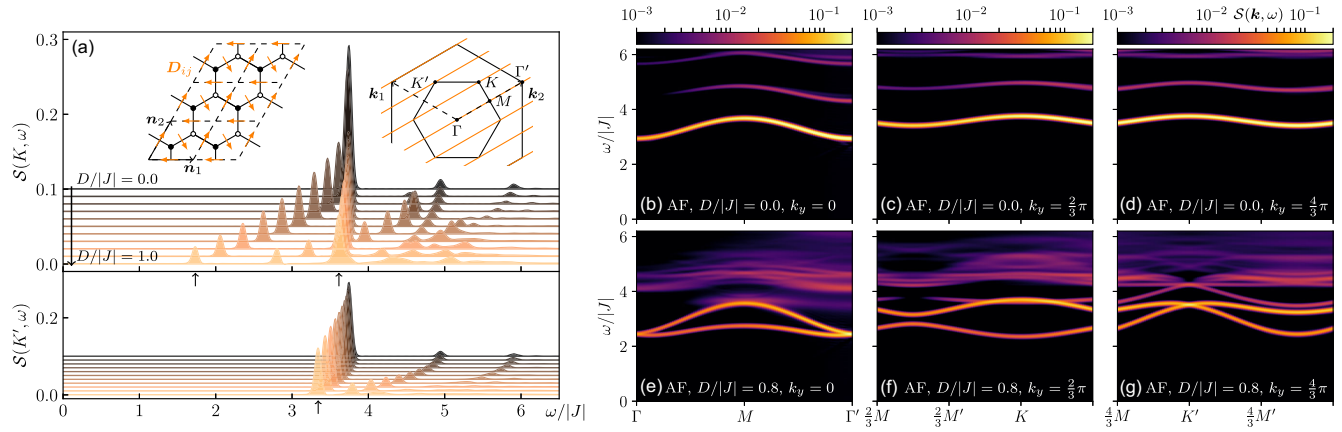

FIG. 2. Dynamical spin-structure factor $\mathcal{S}(\boldsymbol{k},\omega)$ for the spin-1/2 honeycomb lattice antiferromagnet, $J_z/|J| = 2.4$, and DMI obtained by numerically time-evolving a matrix product state [41]. (a) Line plots at the high-symmetry points K (top) and K' (bottom) for increasing DMI from $D/|J| = 0$ to $D/|J| = 1$ illustrate the splitting of the spin wave bands at K while the splitting is absent at K'. Magnon bands are highlighted by arrows. Insets show the lattice and the corresponding momenta lines determined by the cylindrical geometry with six sites circumference. (b)–(g) Representative color plots along aforementioned momenta cuts for zero DMI (top) and $D/|J| = 0.8$ (bottom). The magnon bands (bright yellow features) split across the entire BZ apart from the Γ and K' points that feature Dirac cones.

model without DMI has symmetry group $\mathcal{G}_M^*$ with a U(1) symmetry.

Expanding in fluctuations (sublattice-dependent bosons a and b), one obtains the harmonic Hamiltonian in $\boldsymbol{k}$ space $H_2(J,J_z) = \frac{1}{2}\sum_{\boldsymbol{k}} \boldsymbol{\psi}_{\boldsymbol{k}}^\dagger H_{\boldsymbol{k}} \boldsymbol{\psi}_{\boldsymbol{k}}$, where $H_{\boldsymbol{k}} = \mathrm{diag}(h_{\boldsymbol{k}}, h_{-\boldsymbol{k}})$ in the basis $\boldsymbol{\psi}_{\boldsymbol{k}}^\dagger = (a_{\boldsymbol{k}}^\dagger, b_{-\boldsymbol{k}}, b_{\boldsymbol{k}}^\dagger, a_{-\boldsymbol{k}})$ with

$$h_{\boldsymbol{k}} = \frac{1}{2}\begin{pmatrix} 3J_z & -J\gamma_{\boldsymbol{k}} \\ -J\gamma_{-\boldsymbol{k}} & 3J_z \end{pmatrix}, \qquad \gamma_{\boldsymbol{k}} = \sum_{n=0}^{2} e^{i\boldsymbol{k}\cdot\boldsymbol{\delta}_n}. \tag{2}$$

The nearest neighbor bonds are $\boldsymbol{\delta}_n = (\cos\phi_n, \sin\phi_n)$ with $\phi_n = 2\pi n/3 + \pi/2$. After diagonalization, we find the normal mode magnon energies $\varepsilon_{\boldsymbol{k},\sigma} = \frac{1}{2}\sqrt{(3J_z)^2 - J^2|\gamma_{\boldsymbol{k}}|^2}$, which are twofold spin-degenerate over the entire BZ ($\sigma = \uparrow, \downarrow$). This degeneracy is a result of the spurious U(1) and PT symmetries in the LSWT. They appear because the harmonic theory is blind to the symmetry breaking DMI that enters, to lowest order, to cubic order in the bosons; for a qualitative discussion, see SM [46].

We explore the effects of the DMI by carrying out a real-space perturbation theory [64]. We decompose $H = H_0 + V$ into an unperturbed piece, $H_0 = (J_z/2)\sum_{\langle ij\rangle} S_i^z S_j^z$, and a perturbation V, which includes the other terms in Eq. (1). The ground state $|0\rangle$ of H_0 is the Néel state with fully polarized sublattices. We are interested in the effective Hamiltonian for magnons built from states $|i\rangle$ with a single spin flip (at site i) relative to $|0\rangle$. To second order in V, its matrix elements read [65]

$$H_{ij}^{\mathrm{eff}} = \langle i| \Big[H_0 + V + \frac{1}{2}\sum_v V|v\rangle\langle v|V\left(\frac{1}{E_i - E_v} + \frac{1}{E_j - E_v}\right)\Big] |j\rangle,$$

where $|v\rangle$ labels virtual states with two or more spin flips. See the SM [46] for details. Importantly, processes lifting the band degeneracy are found to second-order in the DMI-induced perturbation $V_D = \frac{1}{2}\sum_{\langle ij\rangle} \boldsymbol{D}_{ij} \cdot \boldsymbol{S}_i \times \boldsymbol{S}_j$ via virtual two-spin-flip states:

$$\frac{-2}{J_z} \left\langle \; i\!\!\bigcirc\!\!-\!\!\bigcirc j \;\middle|\, V_D \,\middle|\; i\!\!\bullet\!\!-\!\!\bigcirc j \;\right\rangle \left\langle \; i\!\!\bullet\!\!-\!\!\bigcirc j \;\middle|\, V_D \,\middle|\; i\!\!\bigcirc\!\!-\!\!\bigcirc j \;\right\rangle \propto \frac{D^2}{J_z} e^{-2i\varphi_{ij}},$$

where $\tan\varphi_{ij} = D_{ij}^y / D_{ij}^x$. The states depict the pattern of spin flips generated by V_D. White (black) circles indicate the ground state (spin flips). Such a coupling mimics the bond-dependent symmetric off-diagonal exchange interaction that breaks spin conservation: $e^{-2i\varphi_{ij}}(D^2/J_z) S_i^+ S_j^+$. Thus, by taking these terms to replace the DMI in Eq. (1), we account for the qualitative effects of DMI. We consider the amended Hamiltonian

$$H' = \sum_{i\in \mathrm{A}} \sum_{j=0}^{2} \Big[J_z S_i^z S_{i+\boldsymbol{\delta}_j}^z + \frac{J}{2}\left(S_i^+ S_{i+\boldsymbol{\delta}_j}^- + S_i^- S_{i+\boldsymbol{\delta}_j}^+\right) + \frac{J'_{++}}{2}\left(e^{i\vartheta_{\delta_j}} S_i^+ S_{i+\boldsymbol{\delta}_j}^+ + e^{-i\vartheta_{\delta_j}} S_i^- S_{i+\boldsymbol{\delta}_j}^-\right)\Big], \tag{3}$$

where $|J'_{++}| \propto D^2/J_z$. The i sum runs over all sites of the A sublattice (spin-up) and the phases along the nearest neighbor bonds read $\vartheta_{\boldsymbol{\delta}_n} = 2\pi n/3$. A LSWT of H' yields a bilinear Hamiltonian $H_2'(J, J_z, D)$ that no longer features a block-diagonal kernel. As a result, the degeneracy of the magnon modes is lifted throughout the BZ except for the Γ and the K' points, which feature magnon Dirac cones, in agreement with Refs. [66,67]; see the SM [46] for details.

The qualitative predictions of the modified LSWT are borne out by a fully nonperturbative calculation on the original model, Eq. (1). Figure 2 shows the dynamical spin-structure factor obtained from DMRG + tMPO; see SM for technical details [46]. Constant momentum slices show the progressive splitting of the bands at K as a function of the DMI coupling [Fig. 2(a)]; in contrast, the magnon bands stay degenerate at K'. As predicted, the DMI lifts the double degeneracy of the single magnon levels almost everywhere in the zone with exceptions at Γ and K', where we find *interaction-induced Dirac magnons* [Figs. 2(b)–2(g)].

For the ferromagnetic analogue of model B ($J_z < J < 0$), symmetry dictates that there should be a topological gap but spurious symmetries at the LSWT level stabilize gapless Dirac points [15]. After implementing the correct symmetries by a perturbation theory, the resulting amended Hamiltonian is the bosonic version of the Haldane model [68]. See the SM for details and a comparison against DMRG + tMPO [46].

Model C: Tetragonal lattice model.—The previous examples were intended to showcase in the simplest possible settings the shell anomaly and anisotropy blindness. We now present an example with highly anisotropic couplings such as one might find in a realistic strong spin-orbit coupled insulating magnet. In this non-fine-tuned model both shell anomaly and anisotropy blindness occur and lead to enhanced symmetry in the LSWT [captured by magnetic group $\mathcal{G}_E^*$ of Fig. 1(a)]. As before, by going to further shells of interactions, the symmetry is lowered to that of the magnetic structure.

We consider a ferromagnetic bipartite lattice with a tetragonal structure described by space group $P4$ (# 75) and Wyckoff position $2c$ $(0, 1/2, z)$ and $(1/2, 0, z)$ [Fig. 3(a)]. This has low symmetry—with only a C_4 rotation around the c (vertical) axis. On the basis of this information alone, one may determine all symmetry-allowed bilinear exchange couplings within a given shell. In the absence of symmetry there are, in principle, nine such couplings on a bond

$$\begin{pmatrix} J_1^{xx} & J_1^{xy} & J_1^{xz} \\ J_1^{yx} & J_1^{yy} & J_1^{yz} \\ J_1^{zx} & J_1^{zy} & J_1^{zz} \end{pmatrix}, \tag{4}$$

and the nearest neighbor shell has low enough symmetry that all nine are allowed. In the second shell, symmetry forbids longitudinal-transverse couplings and antisymmetric exchange giving five exchange parameters in total. These two shells form the minimal strong spin-orbit coupled model (the "$J_1 + J_2$ model") that connects all moments in three dimensions. Anisotropy blindness eliminates a further four couplings leaving 10 in all. We keep all of these exchange parameters to ensure the model has as little symmetry as the anisotropy blindness and shell anomaly allow (see also [38,46]). Representation theory

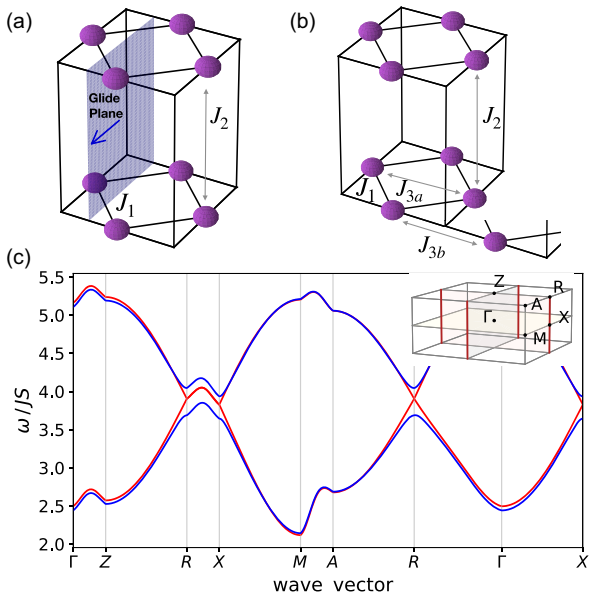

FIG. 3. (a),(b) Space group $P4$ tetragonal lattice. (a) The anisotropic $J_1 + J_2$ exchange model with all nearest and next nearest neighbor couplings has a spurious LSWT symmetry with an anisotropy blindness and shell anomaly enabled glide plane combined with a C_{4z} spin rotation that maps J_{3a} to J_{3b}. (b) Addition of the J_3 couplings breaks this symmetry down. (c) Magnon dispersions above the field-polarized ground state along high symmetry directions (see BZ inset) calculated within LSWT. The $J_1 + J_2$ model (red) features spurious nodal lines, which are lifted switching on the next shell interaction J_3 (blue). The parameters are listed in the SM [46].

leads us to expect a Chern gap in this model [38], which nevertheless is not present in LSWT in the $J_1 + J_2$ model due to an enforced degenerate nodal line on the boundary of the BZ [Fig. 3(c)].

The expected gap is recovered by going to the next shell—the $J_1 + J_2 + J_3$ model [see Fig. 3(b)]. Symmetry has the effect of forbidding only antisymmetric exchange for both inequivalent bonds on the third shell leading to a further 12 couplings and these lift the $J_1 + J_2$ model degeneracy.

The presence of the extra degeneracy in the $J_1 + J_2$ model can be understood in the context of spin-space group representation theory [37,46]. The key enhanced symmetry, present in the LSWT of $J_1 + J_2$, is a glide plane, which is responsible for the nodal line degeneracy. This symmetry is allowed by anisotropy blindness which, in symmetry terms, amounts to a C_2 spin rotation around the c axis. This twofold spin rotation remains trivial for the $J_1 + J_2 + J_3$ model. But in the $J_1 + J_2$ model it combines with the remaining symmetries leading to an enhancement of the symmetries to a spin-space group.

The real-space perturbation theory applied to the previous examples can also be applied here. One may begin with the J_1 model in the Ising limit and perturb in the

anisotropic couplings. In this case, one must extend the calculation to third order in the perturbation V in order to find inequivalent third neighbor couplings that are allowed by the crystal symmetry.

Discussion and symmetry context.—Consider the situation where one wishes to characterize the magnetism of a material from spin wave data. As will be clear from the foregoing, the implementation of symmetries in LSWT contains potential pitfalls. We offer the following practical guide to using LSWT so that no spurious degeneracies arise.

Given a magnetic structure one may enumerate the spin and space locked transformations that leave the structure invariant. These symmetry elements form a magnetic space group $\mathcal{M}$. However, approximations to the full exchange Hamiltonian have the potential to break this locking leading to an enhanced symmetry formally described by spin-space groups [69,70]. There may be physically well-motivated cases where the exchange couplings have spin-space symmetry—for example, in collinear Heisenberg systems, in Kitaev magnets, or generally when spin-orbit coupling is weak and there is a selection in the hierarchy of exchange terms [37]. There may be, in addition, cases where materials themselves realize a shell anomaly as a result of short-ranged couplings, leading to a physically relevant enhanced symmetry within instrumental resolution. This mechanism could be at work in MnF_2 [42,43,46,62,63]. Further high resolution experimental work may be of interest to look for degeneracy breaking in MnF_2.

However, as we have described, there are ways in which the intended symmetries may not be represented faithfully in the excitation spectrum. For example, one may underestimate the range of significant exchange couplings in the material leading to spurious symmetries at the Hamiltonian level. In the case of anisotropy blindness, LSWT itself has a spurious twofold spin rotation symmetry around the magnetization vector for a collinear system that can lead to spin-space symmetries that are absent in the exact theory.

In general, as a practical rule of thumb, one should be especially cautious about LSWT for (i) collinear systems and for (ii) systems where the magnetic lattice has much higher symmetry than the entire crystal (models A, C), and, additionally, in the weak spin-orbit coupling regime when there are important couplings with longitudinal-transverse components (model B) [46]. To realize the desired symmetries in LSWT—whether deliberately enhanced or identical to those of the underlying space group—one may find couplings out to the nth shell that are enforced by the space group of the crystal and work out the symmetry of the ensuing hopping model at each shell by finding the symmetry elements associated with that shell. As an outlook, we emphasize that, where our discussion of the shell anomaly has focused on its realization in spin waves, the ingredients to find it may arise in tight-binding models regardless of the quasiparticle type, thus enlarging the possibility of enhanced symmetries beyond the hydrodynamic regime [71,72].

This work was funded in part by the Deutsche Forschungsgemeinschaft (DFG, German Research Foundation)—Project No. 504261060 (Emmy Noether Programme), SFB 1143 (project-id 247310070) and cluster of excellence ct.qmat (EXC 2147, project-id 390858490). M. G. acknowledges support by JSPS KAKENHI Grant No. 22K14008, by the Theory of Quantum Matter Unit of the Okinawa Institute of Science and Technology Graduate University (OIST), and by the Scientific Computing section of the Research Support Division at OIST for providing the HPC resources.

[1] M. E. Zhitomirsky and A. L. Chernyshev, Colloquium: Spontaneous magnon decays, Rev. Mod. Phys. **85**, 219 (2013).
[2] M. Malki and G. Uhrig, Topological magnetic excitations, Europhys. Lett. **132**, 20003 (2020).
[3] V. Bonbien, F. Zhuo, A. Salimath, O. Ly, A. Abbout, and A. Manchon, Topological aspects of antiferromagnets, J. Phys. D **55**, 103002 (2021).
[4] P. A. McClarty, Topological magnons: A review, Annu. Rev. Condens. Matter Phys. **13**, 171 (2022).
[5] A. V. Chumak, V. I. Vasyuchka, A. A. Serga, and B. Hillebrands, Magnon spintronics, Nat. Phys. **11**, 453 (2015).
[6] T. Holstein and H. Primakoff, Field dependence of the intrinsic domain magnetization of a ferromagnet, Phys. Rev. **58**, 1098 (1940).
[7] O. A. Starykh, A. V. Chubukov, and A. G. Abanov, Flat spin-wave dispersion in a triangular antiferromagnet, Phys. Rev. B **74**, 180403(R) (2006).
[8] A. L. Chernyshev and M. E. Zhitomirsky, Spin waves in a triangular lattice antiferromagnet: Decays, spectrum renormalization, and singularities, Phys. Rev. B **79**, 144416 (2009).
[9] S. Sachdev, *Quantum Phase Transitions* (Cambridge University Press, Cambridge, 2011).
[10] J. Villain, R. Bidaux, J.-P. Carton, and R. Conte, Order as an effect of disorder, J. Phys. **41**, 1263 (1980).
[11] E. Shender, Antiferromagnetic garnets with fluctuationally interacting sublattices, Sov. J. Exp. Theor. Phys. **56**, 178 (1982).
[12] C. L. Henley, Ordering due to disorder in a frustrated vector antiferromagnet, Phys. Rev. Lett. **62**, 2056 (1989).
[13] J. T. Chalker, P. C. W. Holdsworth, and E. F. Shender, Hidden order in a frustrated system: Properties of the Heisenberg Kagomé antiferromagnet, Phys. Rev. Lett. **68**, 855 (1992).
[14] J. G. Rau, P. A. McClarty, and R. Moessner, Pseudo-Goldstone gaps and order-by-quantum disorder in frustrated magnets, Phys. Rev. Lett. **121**, 237201 (2018).
[15] A. Mook, K. Plekhanov, J. Klinovaja, and D. Loss, Interaction-stabilized topological magnon insulator in ferromagnets, Phys. Rev. X **11**, 021061 (2021).
[16] H. Katsura, N. Nagaosa, and P. A. Lee, Theory of the thermal Hall effect in quantum magnets, Phys. Rev. Lett. **104**, 066403 (2010).

[17] Y. Onose, T. Ideue, H. Katsura, Y. Shiomi, N. Nagaosa, and Y. Tokura, Observation of the magnon Hall effect, Science **329**, 297 (2010).

[18] T. Ideue, Y. Onose, H. Katsura, Y. Shiomi, S. Ishiwata, N. Nagaosa, and Y. Tokura, Effect of lattice geometry on magnon Hall effect in ferromagnetic insulators, Phys. Rev. B **85**, 134411 (2012).

[19] L. Zhang, J. Ren, J.-S. Wang, and B. Li, Topological magnon insulator in insulating ferromagnet, Phys. Rev. B **87**, 144101 (2013).

[20] K. A. van Hoogdalem, Y. Tserkovnyak, and D. Loss, Magnetic texture-induced thermal Hall effects, Phys. Rev. B **87**, 024402 (2013).

[21] R. Shindou, R. Matsumoto, S. Murakami, and J.-i. Ohe, Topological chiral magnonic edge mode in a magnonic crystal, Phys. Rev. B **87**, 174427 (2013).

[22] R. Shindou, J.-i. Ohe, R. Matsumoto, S. Murakami, and E. Saitoh, Chiral spin-wave edge modes in dipolar magnetic thin films, Phys. Rev. B **87**, 174402 (2013).

[23] R. Shindou and J.-i. Ohe, Magnetostatic wave analog of integer quantum Hall state in patterned magnetic films, Phys. Rev. B **89**, 054412 (2014).

[24] A. Mook, J. Henk, and I. Mertig, Magnon hall effect and topology in kagome lattices: A theoretical investigation, Phys. Rev. B **89**, 134409 (2014).

[25] A. Mook, J. Henk, and I. Mertig, Edge states in topological magnon insulators, Phys. Rev. B **90**, 024412 (2014).

[26] S. A. Owerre, A first theoretical realization of honeycomb topological magnon insulator, J. Phys. Condens. Matter **28**, 386001 (2016).

[27] R. Chisnell, J. S. Helton, D. E. Freedman, D. K. Singh, R. I. Bewley, D. G. Nocera, and Y. S. Lee, Topological magnon bands in a kagome lattice ferromagnet, Phys. Rev. Lett. **115**, 147201 (2015).

[28] L. Chen, J.-H. Chung, B. Gao, T. Chen, M. B. Stone, A. I. Kolesnikov, Q. Huang, and P. Dai, Topological spin excitations in honeycomb ferromagnet CrI_3, Phys. Rev. X **8**, 041028 (2018).

[29] J. Fransson, A. M. Black-Schaffer, and A. V. Balatsky, Magnon Dirac materials, Phys. Rev. B **94**, 075401 (2016).

[30] A. Mook, J. Henk, and I. Mertig, Tunable magnon Weyl points in ferromagnetic pyrochlores, Phys. Rev. Lett. **117**, 157204 (2016).

[31] B. Xu, T. Ohtsuki, and R. Shindou, Integer quantum magnon Hall plateau-plateau transition in a spin-ice model, Phys. Rev. B **94**, 220403(R) (2016).

[32] P. A. McClarty, X.-Y. Dong, M. Gohlke, J. G. Rau, F. Pollmann, R. Moessner, and K. Penc, Topological magnons in Kitaev magnets at high fields, Phys. Rev. B **98**, 060404(R) (2018).

[33] L. Chen, J.-H. Chung, B. Gao, T. Chen, M. B. Stone, A. I. Kolesnikov, Q. Huang, and P. Dai, Topological spin excitations in honeycomb ferromagnet CrI_3, Phys. Rev. X **8**, 041028 (2018).

[34] B. Yuan, I. Khait, G.-J. Shu, F. C. Chou, M. B. Stone, J. P. Clancy, A. Paramekanti, and Y.-J. Kim, Dirac magnons in a honeycomb lattice quantum XY magnet $CoTiO_3$, Phys. Rev. X **10**, 011062 (2020).

[35] A. Mook, S. A. Díaz, J. Klinovaja, and D. Loss, Chiral hinge magnons in second-order topological magnon insulators, Phys. Rev. B **104**, 024406 (2021).

[36] A. Scheie, P. Laurell, P. A. McClarty, G. E. Granroth, M. B. Stone, R. Moessner, and S. E. Nagler, Dirac magnons, nodal lines, and nodal plane in elemental gadolinium, Phys. Rev. Lett. **128**, 097201 (2022).

[37] A. Corticelli, R. Moessner, and P. A. McClarty, Spin-space groups and magnon band topology, Phys. Rev. B **105**, 064430 (2022).

[38] A. Corticelli, R. Moessner, and P. A. McClarty, Identifying, and constructing, complex magnon band topology, Phys. Rev. Lett. **130**, 206702 (2023).

[39] S. R. White, Density matrix formulation for quantum renormalization groups, Phys. Rev. Lett. **69**, 2863 (1992).

[40] H. N. Phien, G. Vidal, and I. P. McCulloch, Infinite boundary conditions for matrix product state calculations, Phys. Rev. B **86**, 245107 (2012).

[41] M. P. Zaletel, R. S. K. Mong, C. Karrasch, J. E. Moore, and F. Pollmann, Time-evolving a matrix product state with long-ranged interactions, Phys. Rev. B **91**, 165112 (2015).

[42] L. Šmejkal, J. Sinova, and T. Jungwirth, Beyond conventional ferromagnetism and antiferromagnetism: A phase with nonrelativistic spin and crystal rotation symmetry, Phys. Rev. X **12**, 031042 (2022).

[43] L. Šmejkal, J. Sinova, and T. Jungwirth, Emerging research landscape of altermagnetism, Phys. Rev. X **12**, 040501 (2022).

[44] M. Garst, J. Waizner, and D. Grundler, Collective spin excitations of helices and magnetic skyrmions: Review and perspectives of magnonics in non-centrosymmetric magnets, J. Phys. D **50**, 293002 (2017).

[45] K. S. Burch, D. Mandrus, and J.-G. Park, Magnetism in two-dimensional van der Waals materials, Nature (London) **563**, 47 (2018).

[46] See Supplemental Material at http://link.aps.org/supplemental/10.1103/PhysRevLett.131.186702, which includes Refs. [47–59], for further details and additional supporting data.

[47] S. M. Rezende, A. Azevedo, and R. L. Rodríguez-Suárez, Introduction to antiferromagnetic magnons, J. Appl. Phys. **126**, 151101 (2019).

[48] A. B. Harris, D. Kumar, B. I. Halperin, and P. C. Hohenberg, Dynamics of an antiferromagnet at low temperatures: Spin-wave damping and hydrodynamics, Phys. Rev. B **3**, 961 (1971).

[49] R. Verresen, R. Moessner, and F. Pollmann, Avoided quasiparticle decay from strong quantum interactions, Nat. Phys. **15**, 750 (2019).

[50] I. P. McCulloch, Infinite size density matrix renormalization group, revisited, arXiv:0804.2509.

[51] U. Schollwöck, The density-matrix renormalization group in the age of matrix product states, Ann. Phys. (Amsterdam) **326**, 96 (2011).

[52] E. M. Stoudenmire and S. R. White, Minimally entangled typical thermal state algorithms, New J. Phys. **12**, 055026 (2010).

[53] A. Gendiar, R. Krcmar, and T. Nishino, Spherical deformation for one-dimensional quantum systems, Prog. Theor. Phys. **122**, 953 (2009).

[54] G. U. Yule, VII. On a method of investigating periodicities disturbed series, with special reference to Wolfer's sunspot numbers, Phil. Trans. R. Soc. A **226**, 267 (1927).
[55] J. Makhoul, Linear prediction: A tutorial review, Proc. IEEE **63**, 561 (1975).
[56] T. Barthel, U. Schollwöck, and S. R. White, Spectral functions in one-dimensional quantum systems at finite temperature using the density matrix renormalization group, Phys. Rev. B **79**, 245101 (2009).
[57] S. Mühlbauer, B. Binz, F. Jonietz, C. Pfleiderer, A. Rosch, A. Neubauer, R. Georgii, and P. Böni, Skyrmion lattice in a chiral magnet, Science **323**, 915 (2009).
[58] J. H. Han, J. Zang, Z. Yang, J.-H. Park, and N. Nagaosa, Skyrmion lattice in a two-dimensional chiral magnet, Phys. Rev. B **82**, 094429 (2010).
[59] C. Bradley and A. Cracknell, *The Mathematical Theory of Symmetry in Solids* (Oxford University Press, New York, 2009).
[60] L. Šmejkal, A. Marmodoro, K.-H. Ahn, R. Gonzalez-Hernandez, I. Turek, S. Mankovsky, H. Ebert, S. W. D'Souza, O. Šipr, J. Sinova, and T. Jungwirth, Chiral magnons in altermagnetic RuO_2, arXiv:2211.13806 [Phys. Rev. Lett.].
[61] M. Naka, S. Hayami, H. Kusunose, Y. Yanagi, Y. Motome, and H. Seo, Spin current generation in organic antiferromagnets, Nat. Commun. **10**, 4305 (2019).
[62] O. Nikotin, P. A. Lindgård, and O. W. Dietrich, Magnon dispersion relation and exchange interactions in MnF_2, J. Phys. C **2**, 1168 (1969).
[63] M. T. Hutchings, B. D. Rainford, and H. J. Guggenheim, Spin waves in antiferromagnetic FeF_2, J. Phys. C **3**, 307 (1970).
[64] M. E. Zhitomirsky, Real-space perturbation theory for frustrated magnets: Application to magnetization plateaus, J. Phys. Conf. Ser. **592**, 012110 (2015).
[65] C. Cohen-Tannoudji, J. Dupont-Roc, and G. Grynberg, *Atom—Photon Interactions* (Wiley, New York, 1998).
[66] T. Matsumoto and S. Hayami, Nonreciprocal magnons due to symmetric anisotropic exchange interaction in honeycomb antiferromagnets, Phys. Rev. B **101**, 224419 (2020).
[67] R. R. Neumann, A. Mook, J. Henk, and I. Mertig, Thermal Hall effect of magnons in collinear antiferromagnetic insulators: Signatures of magnetic and topological phase transitions, Phys. Rev. Lett. **128**, 117201 (2022).
[68] F. D. M. Haldane, Model for a quantum Hall effect without landau levels: Condensed-matter realization of the "parity anomaly", Phys. Rev. Lett. **61**, 2015 (1988).
[69] W. F. Brinkman and R. J. Elliott, Theory of spin-space groups, Proc. R. Soc. A **294**, 343 (1966).
[70] D. B. Litvin and W. Opechowski, Spin groups, Physica (Amsterdam) **76**, 538 (1974).
[71] H.-H. Lin, L. Balents, and M. P. A. Fisher, Exact SO(8) symmetry in the weakly-interacting two-leg ladder, Phys. Rev. B **58**, 1794 (1998).
[72] A. J. A. James, R. M. Konik, P. Lecheminant, N. J. Robinson, and A. M. Tsvelik, Non-perturbative methodologies for low-dimensional strongly-correlated systems: From non-Abelian bosonization to truncated spectrum methods, Rep. Prog. Phys. **81**, 046002 (2018).